ICCK

Journal of Nonlinear Dynamics and Applications
http://dx.doi.org/10.62762/JNDA.2026.451847

RESEARCH ARTICLE

Check for updates

Organizational Responsiveness in a Three-Dimensional Discrete Model of AI, ESG Disclosure, and Green Supply Chain Collaboration

Fang Sun[1,*]

[1] Department of Business Administration, Dongshin University, Jeollanam-do 58245, Republic of Korea

Abstract

Artificial intelligence (AI) investment, environmental, social, and governance (ESG) disclosure, and green supply chain collaboration increasingly operate as an interconnected corporate sustainability system, yet their relationships are commonly examined through static or approximately linear models. This study develops a bounded three-dimensional discrete nonlinear framework in which firms periodically adjust AI-investment maturity, ESG disclosure quality, and green supply chain collaboration in response to cross-domain benefits and self-limiting organizational costs. The model contributes by separating structural complementarity from organizational responsiveness, allowing the same long-run configuration to remain feasible while its dynamic stability changes with adjustment speed. A logit adaptive rule keeps all states within the open unit interval, while Hill-type functions capture activation thresholds and saturation. Under the baseline calibration, the system exhibits three interior fixed points: stable low- and high-complementarity regimes separated by an unstable intermediate state. Schur-Jury analysis establishes local stability conditions, and Neimark–Sacker analysis shows that the low and high regimes lose stability at distinct responsiveness thresholds, with subcritical and supercritical bifurcations, respectively. Along the high-regime branch, increasing responsiveness generates quasiperiodic motion, intermittent chaotic subwindows, and re-entrant stable period-3 behavior. A positive leading Lyapunov exponent confirms deterministic chaos, while multi-start diagnostics show that quasiperiodic and chaotic dynamics can coexist with a stable period-3 attractor under different initial conditions over part of the parameter range. The findings show that stronger AI-ESG-green-supply-chain complementarity does not imply that faster organizational adjustment is always beneficial. Effective governance must therefore consider not only the strength of cross-domain reinforcement but also the pacing and damping of organizational responses.

Keywords: artificial intelligence investment, ESG disclosure, green supply chain collaboration, organizational responsiveness, multistability.

Submitted: 29 July 2026
Revised: 07 September 2026
Accepted: 08 September 2026
Published: 10 September 2026

Vol. 2, **No.** 3, 2026.
10.62762/JNDA.2026.451847

***Corresponding author:**
Fang Sun
sf2025@dsu.ac.kr

Citation
Sun, F. (2026). Organizational Responsiveness in a Three-Dimensional Discrete Model of AI, ESG Disclosure, and Green Supply Chain Collaboration. *Journal of Nonlinear Dynamics and Applications*, 2(3), 159–176.

1 Introduction

Artificial intelligence (AI) has moved from a specialized analytical technology toward a general organizational infrastructure for prediction, classification, text processing, anomaly detection, and decision support [1, 2]. Its managerial consequences, however, are not reducible to simple automation. AI systems interact with human judgment, routines, data architectures, and governance arrangements, so the same technology can augment organizational capability while also creating new coordination and control problems [3]. These complementarities are especially important when AI is embedded in corporate sustainability systems, where data originate from multiple functions and supply chain partners and where errors can affect disclosure credibility, investment decisions, and interorganizational trust. Secure AI-enabled transformation therefore depends not only on computing resources, but also on data provenance, model validation, privacy protection, auditability, and accountable information sharing [4].

Empirical research increasingly links digital transformation and AI adoption to corporate environmental, social, and governance (ESG) outcomes. Digitalization is associated with stronger ESG performance and disclosure [5, 6]. AI adoption can also support sustainability performance, green investment, and environmental responsibility when it is accompanied by organizational change [7, 8]. Yet these effects are heterogeneous rather than automatic. Enterprise digitization may influence the environmental, social, and governance dimensions differently, while the value of digital resources depends on how firms combine them with complementary organizational capabilities [9, 10]. These findings motivate treating AI-investment maturity as an endogenous organizational state whose sustainability value depends on information and coordination infrastructure.

A parallel literature shows that digital capabilities can strengthen green supply chain activities. Digital capability and AI-enabled analytics facilitate environmental process integration, supplier information exchange, collaborative innovation, and green supply chain collaboration [11, 12]. Their value is greatest when technologies are aligned with concrete green procurement, production, logistics, and partner-coordination practices rather than adopted in isolation [13, 14]. Most existing studies nevertheless retain a one-way or dyadic structure: digital capability affects ESG outcomes, ESG information supports supply chain coordination, or digital supply chain arrangements improve green innovation. This leaves the wider organizational system underexplored, particularly the possibility that the resulting relationships form a closed feedback loop rather than a sequence of independent marginal effects.

The missing reverse link runs from green supply chain collaboration to subsequent AI investment. As collaboration deepens, firms must process larger volumes of supplier-emissions data, logistics information, environmental certifications, lifecycle indicators, product attributes, and regulatory records. This informational complexity raises the marginal value of automated classification, anomaly detection, forecasting, and optimization. The resulting loop is therefore economically plausible: AI investment strengthens ESG information processing; higher-quality ESG disclosure improves the basis for green collaboration; and collaboration creates additional data and coordination demands that increase the return to further AI investment. Evidence that green integration improves environmental and operational performance supports the collaboration mechanism [15, 16], while resource-based and dynamic-capability perspectives explain why value depends on complementary resource bundles and continuing organizational reconfiguration [17, 18].

Closing the loop changes the theoretical problem. A linear mediation model can describe average directional effects, but it cannot determine whether the same structural environment supports multiple self-consistent organizational regimes or whether rapid adjustment destabilizes an otherwise desirable configuration. A nonlinear formulation is appropriate because the modeled complementarities can exhibit threshold activation and diminishing marginal gains, while eco-innovation drivers can interact through feedback rather than independent linear channels [19]. Such reinforcing and restoring forces can generate multistability, threshold dependence, oscillation, and deterministic complexity [20, 21]. A bounded discrete-time representation is particularly suitable because AI budgets, reporting systems, and supplier programs are revised at organizational decision intervals, and because adjustment speed can then be separated from the structural strength of complementarity.

This study develops a bounded three-dimensional discrete nonlinear model linking corporate

AI-investment maturity, ESG disclosure quality, and green supply chain collaboration. It asks three questions: under what conditions can the same structural environment support stable low- and high-complementarity regimes; how does organizational responsiveness alter local stability without changing fixed-point locations; and can sufficiently rapid cross-domain adjustment generate persistent oscillation or deterministic complexity while all states remain economically bounded? The study contributes by endogenizing the complete AI–ESG–green-collaboration feedback loop, separating structural complementarity from adjustment speed through a bounded logit adaptive map, and establishing a reproducible nonlinear evidence chain spanning Schur–Jury stability, Neimark–Sacker normal forms, attraction basins, Lyapunov spectra, branch-aware multi-start diagnostics, deterministic chaos, and verified period-3 behavior. The central implication is that stronger complementarity and faster response are distinct organizational properties: a valuable sustainability architecture may still require pacing and damping to remain dynamically stable.

2 Theoretical Background and Feedback Mechanisms

2.1 Corporate AI investment and ESG information processing

The modeled AI state is corporate AI-investment maturity, defined as the sustained accumulation of financial, technological, data, and organizational resources devoted to AI-enabled capabilities. It includes software and computing infrastructure, but also data engineering, model deployment, employee learning, governance, and integration with business processes. This broader definition is important because organizational value depends on how technology is embedded in routines and complementary capabilities [1–4]. Empirical evidence from manufacturing contexts shows that the joint deployment of AI capability, corporate social responsibility, and green supply chain management significantly enhances sustainable performance, with digital maturity moderating the strength of these complementarities [17]. Sustaining these complementarities over time depends on dynamic capabilities—including the ability to sense sustainability opportunities, seize digital resources, and reconfigure organizational routines—that enable firms to adapt their AI-investment bundle continuously [18]. Accordingly, the modeled state represents the maturity of a sustained investment-capability bundle rather than one-period monetary expenditure.

For ESG applications, AI can lower the cost of processing heterogeneous sustainability information. Machine learning and natural-language processing can classify disclosures, extract environmental indicators, detect anomalies, reconcile records, and support forecasting. More broadly, digitalization is associated with improved ESG reporting and performance [6, 22]. Empirical evidence further emphasizes internal controls, environmental information quality, and resource-allocation channels [23, 24]. Disclosure quality and internal controls remain important mechanisms through which digital transformation affects ESG outcomes [25]. Recent studies continue to associate digital transformation with ESG performance [26, 27], while digitalization has been shown to strengthen the completeness and comparability of sustainability disclosures through internal controls and data standardization mechanisms [22, 25]. Green-AI and Industry 5.0 research highlights the role of technology in improving ESG disclosure processes [28, 29]. Digital transformation can also improve total factor productivity by embedding ESG practices into operational processes [30], while simultaneously shaping the strategic pattern through which firms time and frame their ESG information disclosures [31].

The mechanism is not purely technological. Reliable ESG disclosure requires trustworthy data. Berente et al. [4] and Janssen et al. [32] emphasize data governance and accountability as foundations for trustworthy AI. The broader ESG and CSR literature confirms that a firm's ESG profile is strongly related to its risk, performance, and value, and that information quality is central to how ESG activities translate into organizational outcomes [33]. Organizational AI governance [34] and systematic mapping of AI–ESG research themes [35] further indicate that information quality and accountability are part of the productive infrastructure of AI. Accordingly, the model treats the AI-to-ESG relationship as a saturating positive effect. At low AI-investment maturity, increases in capability can substantially improve information processing. At high AI-investment maturity, the incremental disclosure benefit declines because major automation and integration opportunities have already been captured.

2.2 ESG disclosure and green supply chain collaboration

ESG disclosure is defined here as the quality of sustainability information made available to internal and external stakeholders. Quality includes reliability, completeness, timeliness, comparability, and usefulness rather than the sheer amount of reporting. This distinction matters because symbolic reporting can increase disclosure volume without improving interorganizational coordination.

High-quality ESG information can support green supply chain collaboration in several ways. It clarifies environmental priorities, creates shared metrics, reduces uncertainty about supplier requirements, and provides a basis for joint target setting and monitoring. When partners can observe credible environmental information, they can coordinate green procurement, process redesign, emissions reduction, traceability, and supplier development more effectively [15, 16]. Green supply chain practices also benefit from supply chain traceability and ecocentricity—the degree to which firms embed ecological concerns across their partner network—as moderating conditions that shape how green practices translate into environmental and cost performance [36], while differentiated supplier, customer, and internal integration further amplify sustainable outcomes [37]. Sustainable supply chain research frames such practices as interorganizational responses to environmental and social pressures [38, 39]. Research integrating AI adoption, green finance, and corporate social responsibility shows that green supply chain practices serve as a mediating pathway through which technological and financial sustainability drivers jointly enhance circular economy performance [40, 41].

The effect is again expected to be nonlinear. At very low disclosure quality, additional information may remain too fragmented to influence collaborative behavior. As information becomes sufficiently reliable and standardized, its coordination value can increase quickly. At high disclosure quality, the marginal contribution of additional reporting declines because the main information asymmetries relevant to collaboration have already been reduced. A sigmoidal response captures this activation-and-saturation pattern more naturally than a constant linear coefficient.

2.3 Green supply chain collaboration and the return to AI investment

Green supply chain collaboration refers to coordinated environmental activities between a focal firm and upstream or downstream partners, including environmental information sharing, supplier development, joint target setting, emissions monitoring, green procurement, collaborative innovation, and process improvement. Collaboration is an organizational state rather than a single transaction because its effectiveness depends on repeated information exchange, relational routines, and shared operational standards.

The reverse effect from collaboration to AI investment is central to the proposed model. As green collaboration deepens, the focal firm receives more sustainability data from more nodes; those data become increasingly heterogeneous and time-sensitive, making manual processing costly and increasing the return to automated analytics. Reviews of digital technologies in green supply chain management identify AI, big data, cloud computing, blockchain, and the Internet of Things as complementary enablers [42]. Digital-green cooperation and electronic supply chain collaboration support joint innovation and value co-creation [14, 43]. Big-data analytics capabilities strengthen green supply chain performance through green innovation and technological intensity [44], while Industry 4.0 adoption enhances both environmental and economic performance by enabling and deepening green supply chain management practices [45]. Analytics capabilities can support sustainable advantage [46], while IT capability can strengthen green integration and green innovation [47]. Evolutionary-game and TOE research shows that digital transformation changes low-carbon collaboration incentives under different organizational conditions [48, 49]. Corporate resources and digital supply chain configurations matter when they are aligned with green operational relationships [50, 51]. Big data analytics capability can also unlock green innovation indirectly, with green supply chain integration serving as a key moderating pathway that amplifies the translation of analytical resources into environmental outcomes [52], while firm digitalization is also associated with sustainable innovation performance [53]. Recent AI research evaluates intelligent systems in relation to sustainable supply chain performance [54].

The reinforcing loop is counterbalanced by organizational constraints. The AI-investment state can erode as models, skills, and infrastructure become obsolete. ESG disclosure quality can deteriorate when reporting systems are not maintained or when requirements change. Green collaboration is costly to sustain because suppliers differ in environmental capability, incentives, and data standards. These restoring forces prevent unbounded growth and make multiple equilibria possible.

Taken together, these mechanisms imply a closed reinforcing loop that must coexist with self-limiting organizational forces. The formal model therefore needs to preserve positive cross-domain reinforcement, activation and saturation of complementary benefits, and restoring forces that prevent unchecked expansion.

3 Discrete Nonlinear Model and Methods

3.1 Why a discrete adaptive system?

Corporate AI investment, ESG reporting infrastructure, and interorganizational green programs are not adjusted continuously. Budgets are revised at decision intervals, disclosure systems are updated around reporting cycles, and supplier environmental arrangements are renegotiated through recurring planning and review processes. A discrete-time representation is therefore appropriate when the research question concerns how strongly a firm reacts from one organizational decision cycle to the next. This feedback-oriented treatment is also consistent with system-dynamics research on interacting eco-innovation drivers [19]. More importantly, discrete adjustment separates the strength of complementarity from the speed with which managers react to it: the former determines whether AI, disclosure, and collaboration reinforce one another, while the latter determines whether the resulting system converges smoothly or overshoots.

Let A_t, E_t, and G_t denote corporate AI-investment maturity, ESG disclosure quality, and green supply chain collaboration in decision cycle t. Each state is normalized to the open interval $(0,1)$. The normalization represents organizational maturity rather than a monetary unit and allows the three heterogeneous constructs to be analyzed in a common state space.

Here A_t is a normalized state of sustained AI-investment maturity and associated organizational capability rather than a one-period monetary expenditure. The endpoints 0 and 1 are limiting states, not admissible finite states, because the logit transformation is defined on the open unit interval.

The revised model differs from a conventional Euler discretization. A direct additive update can generate negative capability levels or values above a normalized capacity when responsiveness becomes large. To avoid this problem, adjustment takes place in log-odds space and is mapped back to $(0,1)$ through the logistic function. The resulting map remains smooth and bounded even in the parameter region where bifurcations and chaotic dynamics occur.

Unlike a hard projection onto $[0,1]$, which is nonsmooth at the boundaries and can create artificial boundary sticking, the logit-logistic update remains smooth throughout the admissible state space. For each of the three domains, the marginal response of the next-period state to its corresponding net incentive is $\mu_X X_{t+1}(1-X_{t+1})$; therefore, the same incentive change produces progressively smaller state changes as the state approaches either boundary. This state-dependent attenuation provides a mathematical representation of organizational saturation and friction near capacity limits.

3.2 Nonlinear complementarity and bounded transformation

Cross-domain reinforcement is represented using the Hill function

$$H_X(x) = b_X + (1-b_X)\,\frac{x^{n_X}}{\theta_X^{n_X} + x^{n_X}}. \tag{1}$$

Here, $b_X \in (0,1)$ is baseline activation, $\theta_X \in (0,1)$ is the half-activation point, and $n_X > 1$ controls the steepness of the complementarity. The function is increasing and saturating. It captures the idea that an isolated capability improvement may initially have little effect, that the cross-domain benefit becomes much stronger once complementary infrastructure is present, and that the marginal effect eventually declines.

Define the logistic and logit functions as

$$\sigma(z) = \frac{1}{1+e^{-z}}, \qquad \ell(x) = \ln\left(\frac{x}{1-x}\right). \tag{2}$$

The transformation satisfies $\sigma(\ell(x)) = x$ for every $x \in (0,1)$.

To distinguish behavioral incentives from state updates, define the three net-incentive functions as follows:

$$\Pi_A(A_t, G_t) = r_A + \beta_G H_G(G_t) - c_A A_t, \tag{3a}$$
$$\Pi_E(E_t, A_t) = r_E + \beta_A H_A(A_t) - c_E E_t, \tag{3b}$$
$$\Pi_G(G_t, E_t) = r_G + \beta_E H_E(E_t) - c_G G_t. \tag{3c}$$

Here r_A is the baseline strategic incentive for AI-investment maturity, β_G measures the additional return created by green supply chain collaboration, and c_A captures self-limiting implementation cost, organizational congestion, and the rising burden of sustaining higher AI-investment maturity. The symbols Π_A, Π_E, and Π_G denote net-incentive functions only; Eqs. (4a)–(4c) separately define the next-period states. The A, E, and G subscripts identify the corresponding organizational domain.

3.3 Bounded adaptive map

The bounded three-dimensional state updates are

$$A_{t+1} = \sigma[\ell(A_t) + \mu_A \Pi_A(A_t, G_t)]\,, \tag{4a}$$
$$E_{t+1} = \sigma[\ell(E_t) + \mu_E \Pi_E(E_t, A_t)]\,, \tag{4b}$$
$$G_{t+1} = \sigma[\ell(G_t) + \mu_G \Pi_G(G_t, E_t)]\,. \tag{4c}$$

The parameters μ_A, μ_E, and μ_G are organizational responsiveness coefficients. A small value means that managers adjust gradually even when the net incentive is strong. A large value represents aggressive updating of AI budgets, ESG reporting systems, or supply chain green programs.

Proposition 1 (Invariance of the admissible state space). *For every initial state $(A_0, E_0, G_0) \in (0,1)^3$ and every finite parameter vector satisfying the admissible domains specified in Table 1, Eqs. (4a)–(4c) map $(0,1)^3$ into itself.*

Proof. For any state in $(0,1)^3$, all three logit terms are finite. Under the parameter domains in Table 1, each Hill function and hence each net incentive is finite. The argument of every logistic update is therefore finite, and $0 < \sigma(z) < 1$ for every finite z. Thus $(A_{t+1}, E_{t+1}, G_{t+1}) \in (0,1)^3$. □

This invariance ensures that the complex dynamics analyzed below arise from the feedback mechanism rather than from trajectories leaving the economically meaningful state space.

Table 1 summarizes the variables and parameters, with $X \in \{A, E, G\}$.

Table 1. State variables and parameters of the discrete model.

Symbol	Interpretation	Domain / sign
A_t	Normalized corporate AI-investment maturity	$(0,1)$
E_t	ESG disclosure quality	$(0,1)$
G_t	Green supply chain collaboration	$(0,1)$
r_A, r_E, r_G	Baseline incentives for the three organizational states	> 0
β_G	Reinforcement of AI-investment maturity by green collaboration	> 0
β_A	Reinforcement of ESG disclosure by AI-investment maturity	> 0
β_E	Reinforcement of green collaboration by ESG disclosure	> 0
c_A, c_E, c_G	Self-limiting adjustment cost / organizational friction	> 0
μ_A, μ_E, μ_G	Organizational responsiveness	> 0
b_X	Baseline activation of the Hill function	$(0,1)$
θ_X	Half-activation point	$(0,1)$
n_X	Complementarity steepness	> 1

4 Fixed Points, Local Stability, and Bifurcation Conditions

4.1 Fixed-point system

An interior fixed point $P^\star = (A^\star, E^\star, G^\star)$ is unchanged by the bounded update. Since σ is one-to-one and $\sigma(\ell(x)) = x$, any interior fixed point must satisfy $\Pi_A = \Pi_E = \Pi_G = 0$. The fixed-point conditions are

$$A^\star = \frac{r_A + \beta_G H_G(G^\star)}{c_A}, \tag{5a}$$
$$E^\star = \frac{r_E + \beta_A H_A(A^\star)}{c_E}, \tag{5b}$$
$$G^\star = \frac{r_G + \beta_E H_E(E^\star)}{c_G}. \tag{5c}$$

The adjustment parameters μ_A, μ_E, and μ_G do not change the location of the fixed points. They change only their dynamic stability. This separation is analytically useful and managerially meaningful: identical long-run target configurations can be stable under gradual adjustment but unstable under aggressive adjustment.

Because the Hill functions are sigmoidal, the composite mapping can intersect the identity more than once. A simple sufficient interiority condition is $0 < r_A + \beta_G b_G$ and $r_A + \beta_G < c_A$, together with the analogous inequalities $0 < r_E + \beta_A b_A$, $r_E + \beta_A < c_E$, and $0 < r_G + \beta_E b_E$, $r_G + \beta_E < c_G$. Since each Hill function lies between its baseline activation and one, these inequalities keep every fixed-point component strictly inside the normalized interval. The baseline calibration satisfies the conditions and produces three interior solutions. The lowest and highest are locally stable at moderate responsiveness, whereas the unstable intermediate fixed point helps organize the basin boundary between the two regimes.

4.2 Jacobian and Schur stability

Let

$$\begin{aligned} s_A &= A^\star(1 - A^\star)\,, \\ s_E &= E^\star(1 - E^\star)\,, \\ s_G &= G^\star(1 - G^\star)\,. \end{aligned} \tag{6}$$

At an interior fixed point, differentiation of the bounded logit map gives the cyclic Jacobian

$$J^\star = \begin{pmatrix} d_A & 0 & k_A \\ k_E & d_E & 0 \\ 0 & k_G & d_G \end{pmatrix}. \tag{7}$$

The local restoring terms and cross-domain gains are defined by

$$d_A = 1 - \mu_A c_A s_A, \tag{8a}$$
$$d_E = 1 - \mu_E c_E s_E, \tag{8b}$$
$$d_G = 1 - \mu_G c_G s_G, \tag{8c}$$

$$k_A = \mu_A \beta_G H_G'(G^\star)\, s_A, \tag{9a}$$
$$k_E = \mu_E \beta_A H_A'(A^\star)\, s_E, \tag{9b}$$
$$k_G = \mu_G \beta_E H_E'(E^\star)\, s_G. \tag{9c}$$

This decomposition separates self-damping from feedback amplification and makes the stability mechanism transparent. The characteristic equation is

$$(\lambda - d_A)(\lambda - d_E)(\lambda - d_G) - k_A k_E k_G = 0. \tag{10}$$

The equivalent monic cubic form is

$$\lambda^3 + a_1\lambda^2 + a_2\lambda + a_3 = 0, \tag{11}$$

with coefficients

$$a_1 = -\,(d_A + d_E + d_G)\,, \tag{12a}$$
$$a_2 = d_A d_E + d_A d_G + d_E d_G, \tag{12b}$$
$$a_3 = -\,(d_A d_E d_G + k_A k_E k_G)\,. \tag{12c}$$

Here the sign convention follows the expansion of $\det(\lambda I - J^\star)$, so that a_1 equals the negative of the trace of $J^\star$ and a_3 equals $-\det(J^\star)$, where $\det(J^\star) = d_A d_E d_G + k_A k_E k_G$.

Proposition 2. *For the monic cubic characteristic polynomial in Eq. (11), an interior fixed point is locally asymptotically stable if and only if the four Schur–Jury inequalities (13a)–(13d) below hold. Equivalently, all multipliers of the fixed-point Jacobian lie strictly inside the unit circle. Under the baseline calibration, the low and high fixed points satisfy all four inequalities, whereas the intermediate fixed point violates (13a), consistent with the classification in Table 3.*

Proof. Linearization around an interior fixed point gives the perturbation system $\delta x_{t+1} = J^\star \delta x_t$. Local asymptotic stability is therefore equivalent to every root of $\det(\lambda I - J^\star) = 0$ lying strictly inside the unit disk. Applying the cubic Jury criterion to the monic polynomial in Eq. (11) yields exactly Eqs. (13a)–(13d), so these inequalities are necessary and sufficient. □

$$1 + a_1 + a_2 + a_3 > 0, \tag{13a}$$
$$1 - a_1 + a_2 - a_3 > 0, \tag{13b}$$
$$1 - a_2 + a_1 a_3 - a_3^2 > 0, \tag{13c}$$
$$|a_3| < 1. \tag{13d}$$

The coefficient inequalities make the stability boundary explicit rather than relying only on numerical eigenvalue inspection. They also clarify why responsiveness matters: the three adjustment-speed parameters enter both the local restoring terms and the cross-domain gain terms of the Jacobian. Faster adjustment can therefore move characteristic roots through the unit circle even when the fixed-point locations themselves remain unchanged.

4.3 Neimark–Sacker conditions and normal form

Suppose a scalar continuation parameter μ is imposed by setting $\mu_A = \mu_E = \mu_G = \mu$. A Neimark–Sacker bifurcation occurs at $\mu = \mu_c$ when a complex conjugate pair satisfies

$$\lambda_{1,2}(\mu_c) = e^{\pm i\vartheta_0}, \qquad |\lambda_{1,2}(\mu_c)| = 1, \tag{14}$$

while the third eigenvalue remains inside the unit circle. Standard nonresonance requires

$$\lambda_1^k(\mu_c) \neq 1, \qquad k = 1, 2, 3, 4, \tag{15}$$

and the transversal crossing condition requires

$$\left. \frac{d\,|\lambda_1(\mu)|}{d\mu} \right|_{\mu=\mu_c} \neq 0. \tag{16}$$

Proposition 3 (Generic Neimark–Sacker bifurcation). *Along the synchronized path $\mu_A = \mu_E = \mu_G = \mu$, suppose Eqs. (14)–(16) hold, the third multiplier satisfies $|\lambda_3(\mu_c)| < 1$, and $l_1^{\mathrm{NS}} \neq 0$. Then the interior fixed point undergoes a generic Neimark–Sacker bifurcation at $\mu = \mu_c$. Under the sign convention of Eq. (20), $l_1^{\mathrm{NS}} < 0$ gives a supercritical bifurcation with a locally stable invariant closed curve, whereas $l_1^{\mathrm{NS}} > 0$ gives a subcritical bifurcation with a locally unstable invariant closed curve.*

Proof. Eqs. (14)–(16) provide a simple unit-modulus conjugate pair, the required nonresonance conditions, and transversal crossing. The condition $|\lambda_3| < 1$ excludes an additional critical multiplier, while $l_1^{\mathrm{NS}} \neq 0$ supplies the normal-form nondegeneracy condition. The sign conclusion follows from the reduced map normal form in Eqs. (17)–(20). □

To determine the direction and stability of the bifurcating invariant curve, let q and p denote normalized right and left eigenvectors associated with the critical conjugate multipliers. Specifically, q and p satisfy $J^\star q = e^{i\vartheta_0} q$, $(J^\star)^{\mathsf{H}} p = e^{-i\vartheta_0} p$, and $p^{\mathsf{H}} q = 1$. Let B and C denote the symmetric multilinear forms generated by the second- and third-order derivatives of the map, with $B(u,v) = D^2F(P^\star)[u,v]$ and $C(u,v,w) = D^3F(P^\star)[u,v,w]$ defined without factorial scaling. The auxiliary vectors are then constructed as follows.

$$h_{11} = (I - J^\star)^{-1} B(q,\bar{q})\,, \tag{17a}$$
$$h_{20} = \left(e^{2i\vartheta_0} I - J^\star\right)^{-1} B(q,q). \tag{17b}$$

Following the standard multidimensional Neimark–Sacker normal-form construction [21, 55], the third-order interaction terms are

$$c_{21} = C(q,q,\bar{q})\,, \tag{18a}$$
$$b_{11} = B(q,h_{11})\,, \tag{18b}$$
$$b_{20} = B(\bar{q},h_{20})\,. \tag{18c}$$

The reduced cubic and first Lyapunov coefficients are

$$G_{21} = p^{\mathsf{H}}(c_{21} + 2b_{11} + b_{20})\,, \tag{19}$$
$$l_1^{\mathrm{NS}} = \tfrac{1}{2}\,\mathrm{Re}\left(e^{-i\vartheta_0} G_{21}\right). \tag{20}$$

When the first Lyapunov coefficient is negative, a stable invariant closed curve emerges from a supercritical Neimark–Sacker bifurcation. When it is positive, the bifurcation is subcritical and a nearby unstable invariant closed curve exists on the pre-bifurcation side. This sign convention follows the standard map normal form [21, 55].

For reproducibility, the multilinear forms B and C were obtained by analytic symbolic differentiation of the smooth map and were then evaluated in double precision at each critical fixed point. The right eigenvector q was normalized to $\|q\|_2 = 1$ and phase-fixed so that its first nonzero component was positive real; the left eigenvector p was then scaled to satisfy $p^{\mathsf{H}} q = 1$. Critical responsiveness values were bracketed and solved from $|\lambda_c(\mu)| - 1 = 0$ with absolute and relative tolerances of 10^{-12}. The resulting unit-circle residuals were 9.99×10^{-16} at P_L and 1.22×10^{-15} at P_H. The minimum nonresonance residual over $k = 1, \ldots, 4$ was 0.623761 and 0.909915, respectively; the corresponding transversality rates were 0.155685 and 0.129415. Eigenvector and normalization residuals were below 10^{-15}.

4.4 Lyapunov diagnostic for complex dynamics

Local bifurcation analysis identifies the loss of fixed-point stability, but it does not distinguish quasiperiodic motion from chaotic dynamics farther from the critical point. The numerical analysis therefore computes the full Lyapunov spectrum using QR reorthonormalization. At each iteration, the tangent map is factorized as $J_t Q_t = Q_{t+1} R_t$, and the exponents are obtained from the accumulated diagonal terms in Eq. (21). The Lyapunov-spectrum interpretation follows recent nonlinear-stability analysis [56], while the broader bifurcation framework follows standard dynamical-systems theory [57].

$$\Lambda_i = \lim_{N\to\infty} \frac{1}{N} \sum_{t=0}^{N-1} \ln |R_{ii,t}|\,, \qquad i = 1,2,3. \tag{21}$$

The exponents are ordered from largest to smallest. A positive leading exponent indicates sensitive dependence on initial conditions; a leading exponent close to zero is consistent with quasiperiodic motion on an invariant curve, while an entirely negative spectrum implies contraction toward a periodic orbit or fixed point [20, 21]. Representative values in Table 5 use the fixed high-regime seed $(0.90, 0.87, 0.86)$, 10,000 transient iterations, 100,000 retained iterations, and $Q_0 = I$. The sweep underlying Figure 1(c)–(d) uses the same seed, 4,500 transients, 10,000 retained iterations, $Q_0 = I$, and a responsiveness step of $\Delta\mu = 0.02$.

5 Numerical Results

5.1 Baseline calibration

Table 2. Baseline parameter values.

Parameter	Value	Interpretation
r_A	0.12	Baseline strategic incentive for AI-investment maturity
r_E	0.14	Baseline incentive for ESG disclosure quality
r_G	0.09	Baseline incentive for green collaboration
β_G	0.82	Green collaboration → AI-investment maturity
β_A	0.79	AI-investment maturity → ESG disclosure
β_E	0.85	ESG disclosure → green collaboration
c_A	0.96	Self-limiting AI-investment adjustment cost
c_E	1.00	Self-limiting ESG disclosure cost
c_G	0.98	Self-limiting collaboration cost
b_A, b_E, b_G	0.05	Baseline Hill activation
θ_A	0.49	AI-investment activation midpoint
θ_E	0.53	ESG activation midpoint
θ_G	0.51	Collaboration activation midpoint
n_A, n_E, n_G	4	Complementarity steepness
μ_A, μ_E, μ_G	2.00	Baseline organizational responsiveness

The numerical calibration is designed for mechanism identification rather than structural estimation. Parameter values preserve the theoretical ordering implied by the corporate-sustainability mechanisms, produce nondegenerate fixed points within the admissible state space, and permit the responsiveness parameters to reveal changes in local and global dynamics. The three reinforcement coefficients are comparable but nonidentical, representing a strong closed complementarity loop without imposing exact symmetry. Activation midpoints are centered near intermediate maturity, the Hill exponent creates a distinct but smooth activation threshold, and self-limiting coefficients close to unity provide internal damping. No coefficient should therefore be interpreted as an empirical estimate for a particular country or industry; Section 5.5 perturbs the structural parameters to assess whether the qualitative results depend on this benchmark. The full baseline calibration is reported in Table 2.

5.2 Fixed points and bistability

The fixed-point equations yield three interior solutions:

$$P_L = (0.1736,\ 0.1911,\ 0.1489), \tag{22a}$$
$$P_U = (0.4263,\ 0.4529,\ 0.4218), \tag{22b}$$
$$P_H = (0.8891,\ 0.8666,\ 0.8581). \tag{22c}$$

At the baseline responsiveness $\mu_A = \mu_E = \mu_G = 2$, the low and high fixed points are locally stable. The intermediate point has a real eigenvalue above one and is unstable. Table 3 reports the eigenvalues.

Bistability means that two firms governed by the same structural parameters can converge to very different sustainability configurations. Figure 2(a) displays the two attraction basins in the (A_0, E_0) plane at the representative initial collaboration level $G_0 = 0.45$ and $\mu = 2$. The panel also marks the A–E projections of the low, intermediate, and high fixed points; P_U lies on the numerically estimated basin boundary and helps organize it. Figure 2(b) compares numerically estimated basin boundaries for $G_0 = 0.20$, 0.45, and 0.70. Their systematic downward shift as G_0 rises shows that stronger initial green collaboration lowers the joint AI-investment maturity and ESG-disclosure quality needed to enter the high-complementarity basin. The result therefore rules out a universal one-dimensional AI-investment-maturity threshold: transition depends on the firm's joint initial state.

For reproducibility, each basin panel uses a 201×201 uniform grid over $A_0, E_0 \in [0.001, 0.999]$, with $\mu = 2$ and 400 iterations per initial condition. Each terminal state is assigned to the nearest stable fixed point; across the three reported G_0 values, the maximum terminal distance to its assigned attractor is below 10^{-15}. The displayed boundary is the first change in basin classification along each A_0 grid column and should therefore be interpreted as a numerically estimated basin boundary rather than an analytically traced stable manifold.

5.3 Neimark–Sacker bifurcations

For the one-parameter continuation, we impose $\mu_A = \mu_E = \mu_G = \mu$ as a benchmark synchronization path rather than assuming that the three organizational subsystems adjust at identical speeds in practice. The general model retains distinct responsiveness parameters, whereas joint variation provides a transparent one-dimensional continuation path for

Table 3. Fixed points and local stability at $\mu_A = \mu_E = \mu_G = 2$.

Fixed point	Coordinates $(A^\star, E^\star, G^\star)$	Eigenvalues of $J^\star$	Spectral radius	Stability
P_L	$(0.1736, 0.1911, 0.1489)$	$0.6886 \pm 0.0498i$, 0.7897	0.7897	Stable
P_U	$(0.4263, 0.4529, 0.4218)$	1.3129, $0.1220 \pm 0.6875i$	1.3129	Unstable
P_H	$(0.8891, 0.8666, 0.8581)$	0.8585, $0.7412 \pm 0.0623i$	0.8585	Stable

Table 4. Critical Neimark–Sacker bifurcations.

Fixed point	μ_c	Critical multipliers	ϑ_0	Crossing rate	l_1^{NS} / type
P_L	12.5260	$-0.9501 \pm 0.3119i$; $\lambda_3 = -0.3169$	2.8244	0.1557	8.7561; subcritical
P_H	14.6081	$-0.8905 \pm 0.4550i$; $\lambda_3 = -0.03345$	2.6693	0.1294	-20.2073; supercritical

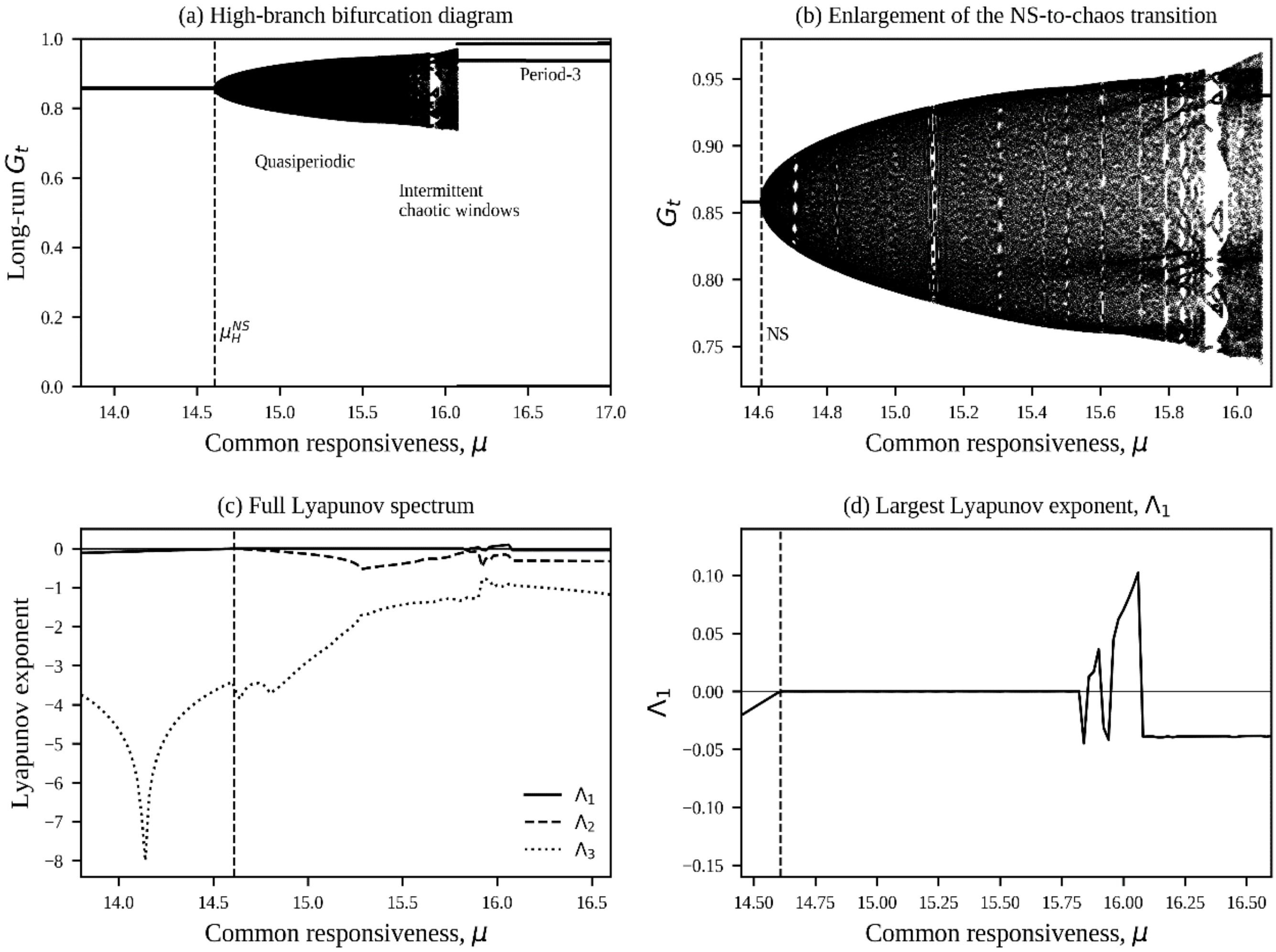

Figure 1. Bifurcation and Lyapunov analysis under increasing organizational responsiveness: (a) high-regime-seeded bifurcation structure of the long-run green-collaboration state; (b) enlargement of the Neimark–Sacker-to-chaos transition; (c) full Lyapunov spectrum; and (d) largest Lyapunov exponent Λ_1.

comparing the local stability and bifurcation behavior of the low- and high-complementarity fixed points. The two fixed points lose stability at different critical values, reported in Table 4.

At the low fixed point, the critical pair is $-0.9501 \pm 0.3119i$, the third multiplier is -0.3169, and the modulus-crossing rate is 0.155685. The positive first Lyapunov coefficient, 8.7561, identifies a subcritical

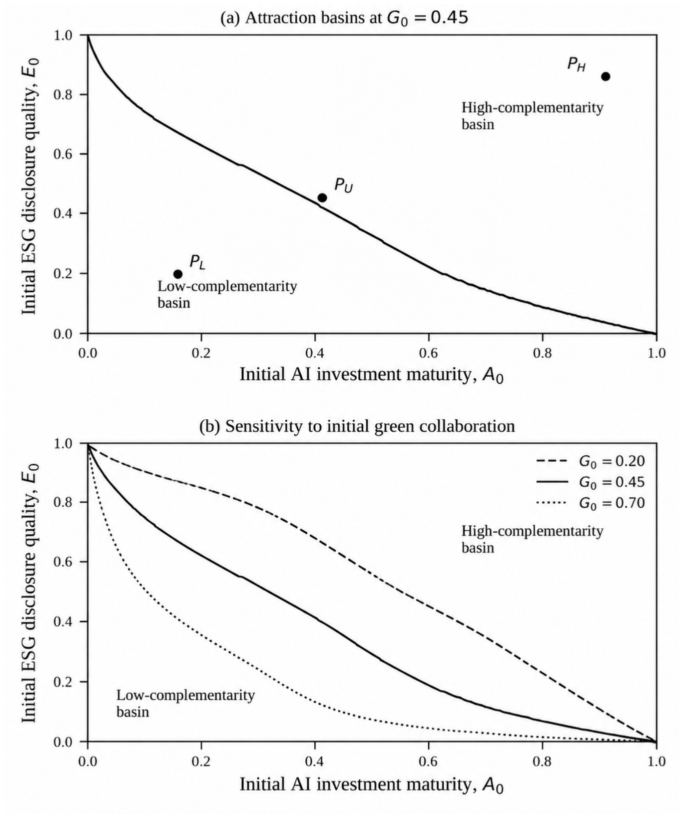

Figure 2. Attraction basins and sensitivity to initial green supply chain collaboration: (a) low- and high-complementarity basins at $G_0 = 0.45$ and $\mu = 2$, with projected fixed-point locations P_L, P_U, and P_H; (b) numerically estimated basin boundaries for $G_0 = 0.20$, 0.45, and 0.70.

Neimark–Sacker bifurcation with a nearby unstable invariant curve on the pre-bifurcation side. At the high fixed point, the critical pair is $-0.8905 \pm 0.4550i$, the third multiplier is -0.03345, and the crossing rate is 0.129415. Here the first Lyapunov coefficient is -20.2073, so the bifurcation is supercritical and produces a stable invariant closed curve. In both cases, the third multiplier lies strictly inside the unit circle, the nonresonance residual is well separated from zero, and the crossing is transversal.

The asymmetry between the two fixed points is theoretically useful. The low-complementarity regime is not simply a scaled-down version of the high regime. It responds differently to acceleration in organizational decision cycles. This means that policies intended to move firms out of a low-sustainability configuration can generate abrupt adjustment rather than a smooth trajectory, whereas excessive responsiveness inside a mature high-complementarity configuration initially produces bounded quasiperiodic oscillation.

5.4 From stable adjustment to quasiperiodicity and chaos

Figure 1(a) traces a high-regime-seeded parameter sweep as common organizational responsiveness increases. For every $\mu \in [13.80, 17.00]$ with $\Delta\mu = 0.002$, the simulation is independently initialized at $(A_0, E_0, G_0) = (0.90, 0.87, 0.86)$, rather than warm-started from the terminal state at the preceding parameter value. Each run discards $4{,}500$ transients and retains 250 iterates for the orbit diagram. Below the high-regime critical value $\mu_H^{\mathrm{NS}} = 14.6081$, trajectories converge to the stable high fixed point. Immediately above the Neimark–Sacker threshold, the fixed point is replaced by a quasiperiodic band associated with an invariant closed curve. Figure 1(b) enlarges the transition region. Near $\mu \approx 16$, intermittent chaotic subwindows are interspersed with narrow regular windows, and at higher responsiveness the high-regime seed converges to a stable period-3 orbit.

Figure 1(c) reports the full Lyapunov spectrum, while Figure 1(d) isolates the leading exponent Λ_1. At the Neimark–Sacker threshold, the two leading exponents approach zero because the critical complex pair lies on the unit circle. At $\mu = 15$, Λ_1 remains numerically close to zero while the remaining exponents are negative, consistent with quasiperiodic motion on a stable invariant curve. At $\mu = 16$, a 10,000-transient/100,000-retained calculation gives approximately $(0.0671, -0.1598, -0.9517)$; the positive leading exponent establishes sensitive dependence on initial conditions and gives a Kaplan–Yorke dimension of approximately 1.42 [20, 56]. At $\mu = 16.5$ and 17.0, all three exponents are negative and the orbit is period-3.

Because the system is multistable, the reported post-bifurcation regimes are not unique global attractors. A deterministic 64-start check using the Cartesian grid $\{0.15, 0.35, 0.65, 0.85\}^3$ was conducted at $\mu = 15$, 16, 16.5, and 17, with $20{,}000$ transients and 600 retained iterates per start. At $\mu = 15$, the two diagonal high-state starts $(0.65, 0.65, 0.65)$ and $(0.85, 0.85, 0.85)$ converged to the high-regime invariant curve, whereas the other 62 starts converged to the coexisting stable period-3 attractor. At $\mu = 16$, the same two high-state starts converged to the high-regime chaotic attractor, while the remaining 62 starts again converged to the stable period-3 attractor. At $\mu = 16.5$ and 17, all 64 tested starts converged to the stable period-3 attractor. The quasiperiodic and chaotic regimes are therefore branch-dependent high-regime dynamics rather than unique global outcomes.

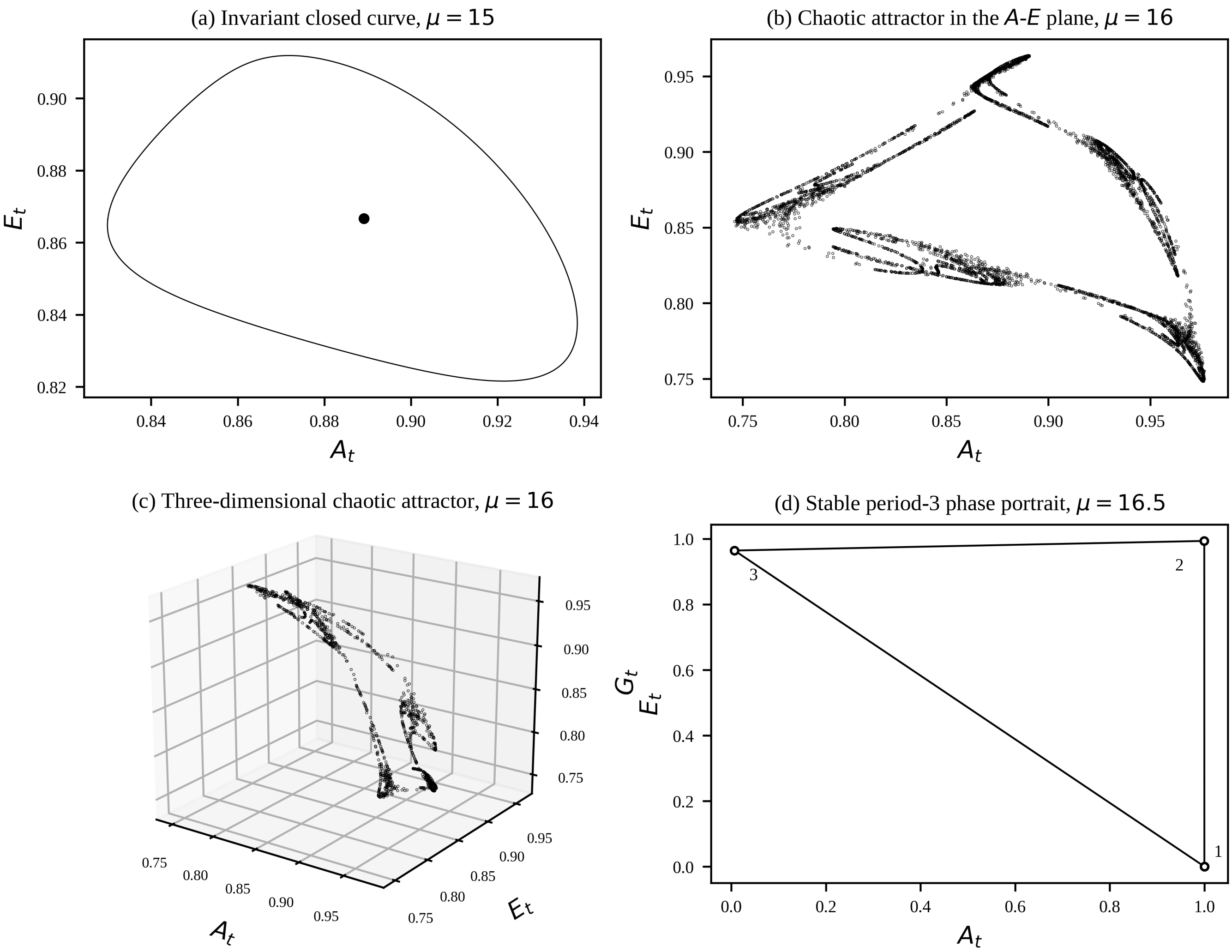

Figure 3. Representative post-bifurcation geometry: (a) quasiperiodic invariant closed curve in the A–E plane at $\mu = 15$; (b) chaotic attractor in the A–E plane at $\mu = 16$; (c) three-dimensional chaotic attractor at $\mu = 16$; and (d) stable period-3 phase portrait in the A–E plane at $\mu = 16.5$.

Table 5. Representative dynamic regimes along the high-regime-seeded branch.

μ	**Lyapunov spectrum** $(\Lambda_1, \Lambda_2, \Lambda_3)$	**Long-run behavior**	**Managerial interpretation**
14.0	$(-0.0818, -0.0818, -4.6489)$	Stable fixed point	Coordinated convergence
14.6081	$(\approx 0, \approx 0, -3.3978)$	Neimark–Sacker threshold	Loss of fixed-point stability
15.0	$(\approx 0, -0.1379, -2.8898)$	Stable invariant closed curve	Persistent quasiperiodic adjustment
16.0	$(0.0671, -0.1598, -0.9517)$; KY dimension ≈ 1.42	Chaotic attractor	Sensitive endogenous irregularity
16.5	$(-0.0389, -0.3199, -1.1187)$	Stable period-3 orbit	Re-entrant regular cycling
17.0	$(-0.0386, -0.3362, -1.7507)$	Stable period-3 orbit	Persistent three-cycle adjustment

Figure 3 compares representative post-bifurcation geometry. Panel (a) shows the stable invariant closed curve at $\mu = 15$ in the A–E plane, with the high fixed point inside the orbit. Panels (b) and (c) show planar and three-dimensional views of the high-regime chaotic attractor at $\mu = 16$. Panel (d) supplies the requested phase portrait for the stable period-3 orbit at $\mu = 16.5$. The three distinct points satisfy $\|F^3(x) - x\|_2 < 10^{-15}$, while $\|F(x) - x\|_2 = 1.36549$ and $\|F^2(x) - x\|_2 = 1.38507$, confirming prime period 3. The multipliers of $D(F^3)$ are 0.889878, 0.382995, and 0.034874, so the spectral radius $0.889878 < 1$

independently confirms asymptotic stability of the three-cycle.

The deterministic chaotic subwindows have a different interpretation from irregularity generated by random external shocks. No stochastic term is introduced into the model. Along the high-regime branch, irregularity is generated endogenously by repeated managerial responses around the AI–ESG–green-collaboration feedback loop. Two nearby trajectories can therefore diverge substantially even when technology, reporting rules, and supply chain conditions remain unchanged.

5.5 Robustness to structural parameters

The principal multistability result persists across the selected one-at-a-time structural perturbations. Perturbations were applied to the three cross-domain reinforcement coefficients, the three activation midpoints, and the three self-limiting cost coefficients, and all tested perturbations preserved three interior fixed points. Varying β_A, β_E, or β_G by $\pm 10\%$ preserved a high-regime Neimark–Sacker boundary, with the first critical responsiveness ranging from approximately 11.09 to 20.52. Varying the three Hill midpoints preserved the same bifurcation type and produced critical values between approximately 12.31 and 17.04.

The self-limiting coefficients affect the type as well as the location of instability. A 10% increase in any of c_A, c_E, or c_G retains a Neimark–Sacker loss of the high fixed point at a lower responsiveness of roughly 10.45–10.79. A 10% reduction in c_A or c_E can make a flip bifurcation occur before the complex pair reaches the unit circle. Within this perturbation set, multistability is robust, whereas the route through which aggressive organizational adjustment becomes unstable depends on the strength of internal damping. The model therefore supports a robust substantive mechanism without implying that every structural parameterization follows the same bifurcation route.

6 Discussion

6.1 Systemic complementarity and dynamic stability

The analysis moves beyond a sequence of marginal relationships. Representative evidence supports links from digitalization to ESG outcomes [5, 6], from digital capability to green supply chain collaboration [11, 12], and from interorganizational digital coordination to collaborative innovation and value co-creation [14]. Big data analytics capability further unlocks green innovation through supply chain integration as a moderating pathway [52]. Sustainable innovation can also contribute to enterprise value and reputation [58, 59]. Closing these links into a feedback system changes the theoretical question: once green collaboration increases the value of future AI investment, the firm operates inside a self-reinforcing organizational system whose long-run state depends on both structural complementarities and adjustment dynamics.

The three fixed points show why firms can remain persistently heterogeneous even under similar external conditions. The low regime is self-consistent: limited AI-investment maturity constrains ESG information processing, weak disclosure reduces the coordination value available to partners, and shallow collaboration in turn reduces the return to further AI investment. The high regime is equally self-consistent but operates through the opposite reinforcement. The intermediate fixed point is unstable and lies on the basin boundary, helping organize the separation between the two attraction regions.

This multistability result strengthens the managerial interpretation of complementarity. A positive coefficient between AI and ESG in a linear model does not imply that a small increase in AI-investment maturity is sufficient to move every firm toward the same long-run outcome. Figure 2 demonstrates that the required change depends on the firm's joint initial state. Initial AI-investment maturity, disclosure quality, and green collaboration can partially compensate for one another in crossing the basin boundary while reinforcing one another in sustaining the high regime.

6.2 The new mechanism: organizational responsiveness

The model also separates fixed-point location from adjustment aggressiveness. The fixed-point coordinates do not depend on μ_A, μ_E, or μ_G, but their stability does. This creates a result that cannot be obtained from a static mediation analysis: faster response can destabilize a desirable high-sustainability configuration without changing the location of the underlying fixed point.

At moderate responsiveness, deviations from the high regime are corrected and the system converges. Along the high-regime branch, once responsiveness reaches the Neimark–Sacker threshold, the correction itself begins to circulate around the feedback loop. AI-investment maturity reacts to green collaboration, ESG systems react to AI-investment maturity, and supply chain arrangements react to ESG information with enough intensity that the state repeatedly overshoots. The system initially remains bounded on an invariant closed curve, while stronger reactions can create branch-dependent endogenous irregularity.

This result offers a nonlinear interpretation of an increasingly common managerial problem. AI-enabled organizations can update forecasts, supplier assessments, risk scores, and sustainability dashboards at much higher frequency than traditional governance processes can absorb. Speed improves information availability, but it can also compress the interval between observation and intervention. When multiple organizational subsystems respond to one another, the relevant question is no longer whether faster information is valuable in isolation. It is whether the entire feedback architecture has sufficient damping to process faster adjustments.

6.3 Quasiperiodicity, chaos, and managerial predictability

The supercritical Neimark–Sacker bifurcation provides a disciplined explanation for persistent oscillation. The system can cease converging while remaining bounded and structured. For managers this means that repeated movements in AI budgets, ESG disclosure intensity, or green supplier collaboration need not indicate implementation failure. They can be an endogenous property of a strongly responsive feedback system.

The high-regime chaotic dynamics at $\mu = 16$ are more consequential. The largest Lyapunov exponent is positive even though the map is deterministic and remains inside the feasible state space. Small differences in organizational states are amplified over time, so long-horizon point forecasts along this branch become unreliable even when the behavioral rules are known. The multi-start analysis also shows that this chaotic attractor can coexist with a stable period-3 attractor, making initial-state dependence an additional source of predictability limits.

The result should not be interpreted as a claim that real firms literally follow the reported numerical calibration. Its value is theoretical: it demonstrates a feasible mechanism through which AI-enabled sustainability systems can become endogenously difficult to predict. The model therefore provides a formal warning against assuming that stronger digital responsiveness always increases control.

6.4 Managerial implications

Managers should treat responsiveness as a design variable. The objective should not be to maximize the speed at which every subsystem reacts. AI investment decisions, ESG reporting changes, and supplier environmental programs operate on different organizational clocks. A governance architecture that forces all three to respond immediately to one another can reduce damping and increase the risk of oscillation.

Illustrative pacing mechanisms consistent with the model include staged AI budgets, rolling rather than instantaneous model deployment, ESG-data validation gates, and supplier-transition periods that reduce effective responsiveness. Such mechanisms do not weaken the underlying complementarity; they alter the speed with which it propagates through the system. This distinction is consistent with the broader requirement for data governance, traceability, model validation, and accountable information sharing that effective AI management demands [4]. Governance can create stability not only by improving data quality but also by preventing rapid feedback from being converted into equally rapid operational changes.

A second implication concerns the weakest link. Strong AI-to-ESG and ESG-to-collaboration effects do not guarantee a stable high regime when self-limiting mechanisms are weak. The robustness analysis shows that changing internal damping coefficients can change the route to instability from a Neimark–Sacker bifurcation to a flip bifurcation. Managers should therefore monitor both cross-domain benefits and the organizational frictions that slow adjustment. In this context, some friction is stabilizing rather than inefficient.

A third implication is diagnostic. Firms approaching a local stability boundary may observe longer adjustment cycles, persistent oscillation, and growing sensitivity to small interventions before the system enters a highly irregular regime. Monitoring the eigenstructure of an empirically calibrated model is unrealistic for most managers, but rising persistence and oscillatory response across AI, reporting, and supplier programs can be interpreted as model-implied early-warning indicators that the feedback loop is becoming too responsive.

6.5 Policy implications

Policy interventions aimed at AI adoption, ESG disclosure, and green supply chains are often designed separately. The model suggests that their combined timing matters. Simultaneously accelerating digital investment, disclosure requirements, and supplier environmental adjustment may generate a stronger response than the sum of the individual policies. When firms already operate near a stability boundary, synchronized acceleration can produce overshooting rather than smooth improvement.

This does not imply that regulators should slow sustainability transitions. It implies that capability-building and adjustment deadlines should be coordinated. Policies that improve data interoperability, verification capability, supplier readiness, and governance capacity increase the system's ability to absorb faster adjustment. The distinction between structural reinforcement and responsiveness also helps explain why identical reporting deadlines or digitalization incentives can generate heterogeneous outcomes across firms with different initial capabilities.

7 Conclusions

This study develops a bounded discrete nonlinear model of AI-investment maturity, ESG disclosure, and green supply chain collaboration. The model retains the central idea that the three organizational states form a reinforcing loop, while making explicit a second mechanism that static formulations cannot represent: organizations differ not only in the strength of their complementarities but also in the speed with which they react to them.

Five conclusions emerge. First, the system supports multiple interior fixed points: low- and high-complementarity regimes can both be stable under the same structural parameters, with an unstable intermediate fixed point on the basin boundary. Second, bounded logit adaptation keeps all states economically feasible even when responsiveness becomes large. Third, the low and high regimes have distinct local bifurcation thresholds and normal-form directions. Fourth, the high regime loses stability through a supercritical Neimark–Sacker bifurcation and gives rise to a stable invariant closed curve. Fifth, the high-regime-seeded sweep develops intermittent chaotic subwindows with a positive leading Lyapunov exponent before converging to a stable period-3 orbit at higher responsiveness; multi-start diagnostics show that the quasiperiodic and chaotic regimes coexist with a stable period-3 attractor over part of the parameter range.

The central managerial implication is therefore not that firms should reduce AI investment or sustainability ambition. It is that strong complementarity and fast adjustment are different properties. A firm can benefit from a strong AI–ESG–green collaboration architecture while still requiring pacing, validation, and governance mechanisms that prevent the feedback loop from reacting too aggressively.

The analysis remains theoretical and mechanism-oriented. The reported parameter values are not structural estimates, and the three state variables aggregate heterogeneous technologies, reporting practices, and supply chain arrangements. Future work could calibrate the model using panel measures of corporate AI investment, ESG disclosure quality, supplier environmental integration, or repeated organizational surveys. A second extension could allow asynchronous decision cycles by estimating separate μ_A, μ_E, and μ_G parameters. Network versions could represent heterogeneous suppliers explicitly, while stochastic extensions could distinguish endogenous deterministic complexity from exogenous environmental shocks.

Despite these limitations, the discrete model changes the interpretation of AI-enabled sustainability transformation. The relevant question is not only whether AI investment improves ESG disclosure or whether disclosure strengthens green collaboration. It is whether the complete feedback system converges, oscillates, or becomes dynamically unpredictable under the organization's actual adjustment speed. That distinction provides a nonlinear systems foundation for understanding why technologically capable firms can still experience unstable sustainability transitions.

Data Availability Statement

Data will be made available on request.

Funding

This work was supported without any funding.

Conflicts of Interest

The author declares no conflicts of interest.

AI Use Statement

The author declares that no generative AI was used in the preparation of this manuscript.

Ethical Approval and Consent to Participate

Not applicable.

References

[1] Verhoef, P. C., Broekhuizen, T., Bart, Y., Bhattacharya, A., Dong, J. Q., Fabian, N., & Haenlein, M. (2021). Digital transformation: A multidisciplinary reflection and research agenda. *Journal of Business Research, 122*, 889-901. [CrossRef]

[2] Dwivedi, Y. K., Hughes, L., Ismagilova, E., Aarts, G., Coombs, C., Crick, T., ... & Williams, M. D. (2021). Artificial Intelligence (AI): Multidisciplinary perspectives on emerging challenges, opportunities, and agenda for research, practice and policy. *International journal of information management, 57*, 101994. [CrossRef]

[3] Raisch, S., & Krakowski, S. (2021). Artificial intelligence and management: The automation–augmentation paradox. *Academy of management review, 46*(1), 192-210. [CrossRef]

[4] Berente, N., Gu, B., Recker, J., & Santhanam, R. (2021). Managing artificial intelligence. *MIS quarterly, 45*(3), 1433-1450. [CrossRef]

[5] Xie, X., Zhu, H., & Zhao, J. (2024). How effective is digital transformation? Heterogeneous insights from listed companies' ESG performance. *Humanities and Social Sciences Communications, 11*(1), 1534. [CrossRef]

[6] Sun, Y., Wu, J., Huang, T. K., Davey, H., & Lu, Y. (2026). Is ESG transparency the fruit of corporate digitalization: Strategic pathways to enhanced ESG disclosure? *Business Strategy and the Environment, 35*(3), 3923-3951. [CrossRef]

[7] Li, J., & Jin, X. (2024). The impact of artificial intelligence adoption intensity on corporate sustainability performance: The moderated mediation effect of organizational change. *Sustainability, 16*(21), 9350. [CrossRef]

[8] Akram, R., Shi, X., Khalid, F., & Srivastava, M. (2025). Artificial intelligence (AI) adoption and green investment: Driving corporate environmental responsibility. *Business Strategy and the Environment, 34*(7), 9188-9202. [CrossRef]

[9] Fang, M., Nie, H., & Shen, X. (2023). Can enterprise digitization improve ESG performance? *Economic Modelling, 118*, 106101. [CrossRef]

[10] Zhong, Y., Zhao, H., & Yin, T. (2023). Resource bundling: How does enterprise digital transformation affect enterprise ESG development? *Sustainability, 15*(2), 1319. [CrossRef]

[11] Cheng, W., Li, Q., Wu, Q., Ye, F., & Jiang, Y. (2024). Digital capability and green innovation: The perspective of green supply chain collaboration and top management's environmental awareness. *Heliyon, 10*(11), e32290. [CrossRef]

[12] Benzidia, S., Makaoui, N., & Bentahar, O. (2021). The impact of big data analytics and artificial intelligence on green supply chain process integration and hospital environmental performance. *Technological Forecasting and Social Change, 165*, 120557. [CrossRef]

[13] Lerman, L. V., Benitez, G. B., Müller, J. M., de Sousa, P. R., & Frank, A. G. (2022). Smart green supply chain management: A configurational approach to enhance green performance through digital transformation. *Supply Chain Management: An International Journal, 27*(7), 147-176. [CrossRef]

[14] Al-Omoush, K. S., de Lucas, A., & del Val, M. T. (2023). The role of e-supply chain collaboration in collaborative innovation and value co-creation. *Journal of Business Research, 158*, 113647. [CrossRef]

[15] Vachon, S., & Klassen, R. D. (2008). Environmental management and manufacturing performance: The role of collaboration in the supply chain. *International Journal of Production Economics, 111*(2), 299-315. [CrossRef]

[16] Wong, C. Y., Wong, C. W., & Boon-itt, S. (2020). Effects of green supply chain integration and green innovation on environmental and cost performance. *International journal of production research, 58*(15), 4589-4609. [CrossRef]

[17] Ying, Z., Chang, T. C., Moslehpour, M., Ismail, S., & Pardaev, J. (2026). Driving Sustainability Through CSR, Artificial Intelligence, and Green Supply Chain; The Role of Green Innovation Capabilities & Digital Maturity. *Corporate Social Responsibility and Environmental Management*. [CrossRef]

[18] Feroz, A. K., Zo, H., Eom, J., & Chiravuri, A. (2023). Identifying organizations' dynamic capabilities for sustainable digital transformation: A mixed methods study. *Technology in Society, 73*, 102257. [CrossRef]

[19] Arranz, C. F. A. (2024). A system dynamics approach to modelling eco-innovation drivers in companies: Understanding complex interactions using machine learning. *Business Strategy and the Environment, 33*(5), 4456-4479. [CrossRef]

[20] Strogatz, S. H. (2018). *Nonlinear dynamics and chaos: With applications to physics, biology, chemistry, and engineering* (2nd ed.). CRC Press. [CrossRef]

[21] Kuznetsov, Y. A. (1998). *Elements of applied bifurcation theory*. New York, NY: Springer New York. https://research-portal.uu.nl/en/publications/elements-of-applied-bifurcation-theory/

[22] Lu, Y., Xu, C., Zhu, B., & Sun, Y. (2024). Digitalization transformation and ESG performance: Evidence from China. *Business Strategy and the Environment, 33*(2), 352-368. [CrossRef]

[23] Wang, L., & Hou, S. (2024). The impact of digital transformation and earnings management on ESG performance: evidence from Chinese listed enterprises. *Scientific Reports, 14*(1), 783. [CrossRef]

[24] Liu, Z., Chen, Z., & Hu, L. (2024). Can enterprise

digital transformation improve ESG performance?. *Managerial and Decision Economics, 45*(7), 5088-5103. [CrossRef]

[25] Zhang, H., Liu, J., & Jiang, H. (2025). The impact of enterprise digital transformation on ESG performance: Evidence from China. *Managerial and Decision Economics, 46*(5), 3157-3171. [CrossRef]

[26] Liu, H., Zhang, X., & He, Y. (2025). Digital transformation and ESG performance: Empirical evidence from Chinese listed companies. *Sustainability, 17*(13), 6165. [CrossRef]

[27] Wang, L., Kong, L., & Zeng, H. (2026). Firm digitalisation empowers ESG performance-evidence from China. *International Journal of Finance & Economics, 31*(2), 1860-1879. [CrossRef]

[28] Rauf, F. (2026). Green AI adoption and ESG disclosure quality: The role of audit committee gender diversity. *Corporate Social Responsibility and Environmental Management*. Advance online publication. [CrossRef]

[29] Asif, M., Searcy, C., & Castka, P. (2023). ESG and Industry 5.0: The role of technologies in enhancing ESG disclosure. *Technological Forecasting and Social Change, 195*, 122806. [CrossRef]

[30] Ding, X., Sheng, Z., Appolloni, A., Shahzad, M., & Han, S. (2024). Digital transformation, ESG practice, and total factor productivity. *Business Strategy and the Environment, 33*(5), 4547-4561. [CrossRef]

[31] He, Y., Li, J., & Ren, Y. (2024). Digital transformation and corporate ESG information disclosure herd effect. *Finance Research Letters, 65*, 105557. [CrossRef]

[32] Janssen, M., Brous, P., Estevez, E., Barbosa, L. S., & Janowski, T. (2020). Data governance: Organizing data for trustworthy artificial intelligence. *Government Information Quarterly, 37*(3), 101493. [CrossRef]

[33] Gillan, S. L., Koch, A., & Starks, L. T. (2021). Firms and social responsibility: A review of ESG and CSR research in corporate finance. *Journal of corporate finance, 66*, 101889. [CrossRef]

[34] Mäntymäki, M., Minkkinen, M., Birkstedt, T., & Viljanen, M. (2022). Defining organizational AI governance. *AI and Ethics, 2*(4), 603-609. [CrossRef]

[35] Wu, Q., Khattak, M. S., Anwar, M., & Nevries, P. (2026). Artificial intelligence and environmental, social, and governance: A hybrid bibliometric approach. *Business Strategy and the Environment, 35*(4), 5749-5775. [CrossRef]

[36] Cousins, P. D., Lawson, B., Petersen, K. J., & Fugate, B. (2019). Investigating green supply chain management practices and performance. *International Journal of Operations & Production Management, 39*(5), 767-786. [CrossRef]

[37] Han, Z., & Huo, B. (2020). The impact of green supply chain integration on sustainable performance. *Industrial Management & Data Systems, 120*(4), 657-674. [CrossRef]

[38] Seuring, S., & Müller, M. (2008). From a literature review to a conceptual framework for sustainable supply chain management. *Journal of Cleaner Production, 16*(15), 1699-1710. [CrossRef]

[39] Zhu, Q., Sarkis, J., & Geng, Y. (2005). Green supply chain management in China: Pressures, practices and performance. *International Journal of Operations & Production Management, 25*(5), 449-468. [CrossRef]

[40] Zhao, J., Ragmoun, W., Dong, Z., Nawaz, M. A., & Sattarov, A. (2026). Circular economy implementation through AI adoption, CSR and green finance: The mediating role of green product innovation and green supply chain. *Corporate Social Responsibility and Environmental Management, 33*(2), 2432-2447. [CrossRef]

[41] Liu, X., Chau, K. Y., Chang, T. C., & Moslehpour, M. (2026). Driving sustainable performance through green business strategy, artificial intelligence capability, and green supply chain management: the mediating roles of knowledge integration and green innovation. *Corporate Social Responsibility and Environmental Management, 33*(3), 4531-4546. [CrossRef]

[42] Wang, Y., Yang, Y., Qin, Z., Yang, Y., & Li, J. (2023). A literature review on the application of digital technology in achieving green supply chain management. *Sustainability, 15*(11), 8564. [CrossRef]

[43] Wang, S., & Zhang, H. (2024). Inter-organizational cooperation in digital green supply chains: A catalyst for eco-innovations and sustainable business practices. *Journal of Cleaner Production, 472*, 143383. [CrossRef]

[44] Al-Khatib, A. W. (2022). Big data analytics capabilities and green supply chain performance: investigating the moderated mediation model for green innovation and technological intensity. *Business Process Management Journal, 28*(5-6), 1446-1471. [CrossRef]

[45] Umar, M., Khan, S. A. R., Yusoff Yusliza, M., Ali, S., & Yu, Z. (2022). Industry 4.0 and green supply chain practices: an empirical study. *International Journal of Productivity and Performance Management, 71*(3), 814-832. [CrossRef]

[46] Behl, A., Gaur, J., Pereira, V., Yadav, R., & Laker, B. (2022). Role of big data analytics capabilities to improve sustainable competitive advantage of MSME service firms during COVID-19–A multi-theoretical approach. *Journal of Business Research, 148*, 378-389. [CrossRef]

[47] Abbas, A., Luo, X., Shahzad, F., & Wattoo, M. U. (2023). Optimizing organizational performance in manufacturing: The role of IT capability, green supply chain integration, and green innovation. *Journal of Cleaner Production, 423*, 138848. [CrossRef]

[48] Li, G., Yu, H., & Lu, M. (2022). Low-carbon collaboration in the supply chain under digital transformation: An evolutionary game-theoretic analysis. *Processes, 10*(10), 1958. [CrossRef]

[49] Li, W., Xiao, X., Yang, X., & Li, L. (2023). How does digital transformation impact green supply chain development? An empirical analysis based on the TOE theoretical framework. *Systems, 11*(8), 416. [CrossRef]

[50] Bae, H. S., & Dong, J. X. (2026). Relationships between corporate resources, green supply chain collaboration and environmental performance. *Benchmarking: An International Journal*, 1-19. [CrossRef]

[51] Roberto, F. R. A., Lerman, L. V., & Benitez, G. B. (2026). Configuring digital supply chains for green supply chain management. *Journal of Manufacturing Technology Management, 37*(3), 599-619. [CrossRef]

[52] Song, M., Yang, M. X., Zeng, K. J., Wang, C., & Wang, F. (2026). Unlocking green innovation through big data analytics capability: A moderated mediation model of green supply chain integration and green leadership style. *Business Strategy and the Environment*. Advance online publication. [CrossRef]

[53] Ardito, L. (2023). The influence of firm digitalization on sustainable innovation performance and the moderating role of corporate sustainability practices: An empirical investigation. *Business Strategy and the Environment, 32*(8), 5252-5272. [CrossRef]

[54] Daios, A., & Kostavelis, I. (2026). Artificial intelligence and sustainable supply chain performance: A trade-off-aware evaluation framework. *Sustainability, 18*(12), 5907. [CrossRef]

[55] Elaydi, S. (2005). *An introduction to difference equations* (3rd ed.). Springer. [CrossRef]

[56] Margazoglou, G., & Magri, L. (2023). Stability analysis of chaotic systems from data. *Nonlinear Dynamics, 111*(9), 8799-8819. [CrossRef]

[57] Hale, J. K., & Koçak, H. (1991). *Dynamics and bifurcations*. Springer. [CrossRef]

[58] Eccles, R. G., Ioannou, I., & Serafeim, G. (2014). The impact of corporate sustainability on organizational processes and performance. *Management science, 60*(11), 2835-2857. [CrossRef]

[59] Flammer, C. (2015). Does corporate social responsibility lead to superior financial performance? A regression discontinuity approach. *Management science, 61*(11), 2549-2568. [CrossRef]